Science of the Total Environment 618 (2018) 121–131

Contents lists available at ScienceDirect

Science of the Total Environment

journal homepage: www.elsevier.com/locate/scitotenv

Stable isotope evidences for identifying crop water uptake in a typical winter wheat–summer maize rotation field in the North China Plain

Xin Zhao [a,b,c], Fadong Li [a,b,*], Zhipin Ai [d], Jing Li [a], Congke Gu [a,b]

[a] Key Laboratory of Ecosystem Network Observation and Modeling, Institute of Geographic Sciences and Natural Resources Research, Chinese Academy of Sciences, Beijing 100101, China
[b] College of Resources and Environment, University of Chinese Academy of Sciences, Beijing 100190, China
[c] Center for Global Environmental Research, National Institute for Environmental Studies, Tsukuba 305-8506, Japan
[d] Center for Regional Environmental Research, National Institute for Environmental Studies, Tsukuba 305-8506, Japan

HIGHLIGHTS

- A full crop water uptake diagram was obtained for winter wheat and summer maize.
- Stable isotope and hierarchical cluster analysis were used to classify soil layers.
- Dry root weight density negatively corresponded to wheat's water uptake.
- Soil water content positively corresponded to both wheat and maize's water uptake.
- Irrigation should be suspended from the booting to flowering stages of wheat.

GRAPHICAL ABSTRACT

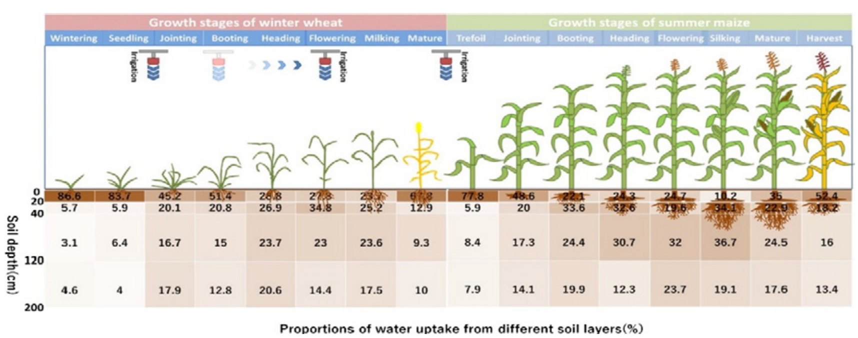

ARTICLE INFO

Article history:
Received 5 August 2017
Received in revised form 26 October 2017
Accepted 30 October 2017
Available online 10 November 2017

Editor: G Ashantha Goonetilleke

Keywords:
Crop water use
$\delta^{18}O$ and $\delta^{2}H$
Dry root weight density
Soil volumetric water content
Irrigation management

ABSTRACT

Better managing agricultural water resources, which are increasingly stressed by climate change and anthropogenic activities, is difficult, particularly because of variations in water uptake patterns associated with crop type and growth stage. Thus, the stable isotopes $\delta^{18}O$ and $\delta^{2}H$ were employed to investigate the water uptake patterns of a summer maize (*Zea mays* L.) and winter wheat (*Triticum aestivum* L.) rotation system in the North China Plain. Based on the soil water content, soil layers were divided into four groups (0–20 cm, 20–40 cm, 40–120 cm, and 120–200 cm) using a hierarchical cluster analysis. The main soil layer of water uptake for summer maize was from 0–20 cm at the trefoil (77.8%) and jointing (48.6%) stages to 20–40 cm at the booting (33.6%) and heading (32.6%) stages, became 40–120 cm at the silking (32.0%) and milking (36.7%) stages, and then returned to 0–20 cm at the mature (35.0%) and harvest (52.4%) stages. Winter wheat most absorbed water from the 0–20 cm soil water at the wintering (86.6%), seedling (83.7%), jointing (45.2%), booting (51.4%), heading (28.8%), and mature (67.8%) stages, but it was 20–40 cm at the flowering (34.8%) and milking (25.2%) stages. The dry root weight density was positively correlated with the contributions of the water uptake for winter wheat. However, no similar correlation was found in summer maize. Regression analysis indicated that the soil volumetric water content (SVWC) was negatively correlated with the contribution of the water uptake (CWU) for summer maize ($CWU = -0.91 \times SVWC + 57.75$) and winter wheat ($CWU = -2.03 \times SVWC + 92.73$). These different responses to water uptake contributions suggested that a traditional irrigation event should be postponed from the booting to flowering stage of winter wheat. This study provides insights into crop water uptake and agricultural water management.

* Corresponding author at: 11A, Datun Road, Chaoyang District, Beijing 100101, China.
E-mail address: lifadong@igsnrr.ac.cn (F. Li).

https://doi.org/10.1016/j.scitotenv.2017.10.315
0048-9697/

1. Introduction

Agriculture, commonly a large water-consumption sector, is now facing increasingly greater challenges because of the water scarcity caused by irrational anthropogenic activities and climate change (Wang et al., 2014; Zipper et al., 2015). This is affecting many regions around the world, such as Southern and Eastern Africa, the Middle East, North-West India, South-West America, and Northern China (Rijsberman, 2006). Thus, several studies have been conducted to reduce field evapotranspiration, to improve agricultural water use efficiency, and to develop water-saving technologies. However, the physiological characteristics of crop water uptake remain largely unclear, especially the variation over crop growth stages. Thus, a better understanding of the sources and magnitudes of crop water uptake can greatly help in making optimal reasonable irrigation schemes for better agricultural water management.

As a major grain producing area, the North China Plain (NCP) produces >50% of the wheat yields and ~40% of the maize yields in China (Mo et al., 2016). Correspondingly, a winter wheat–summer maize rotation is the main cropping system in the NCP (Fang et al., 2010). However, these two crops have distinct water uptake patterns (Ma and Song, 2016; Wang et al., 2010; Zhang et al., 2011) because of their unique traits, including their phenological resources utilizations and root systems. Traditional methods used to determine crops water uptake are based on phenological traits or rooting systems (Draye et al., 2010; Fang et al., 2010; Guan et al., 2015; Qiu et al., 2008). However, they have the disadvantages of not identifying the water source and lacking a quantified estimation of each water source, temporally and spatially (Ehleringer and Dawson, 1992). Instead, a stable isotopes (δ^{18}O and δ^{2}H) method can be employed to reveal water uptake patterns with the apparent advantages of being non-destructive and accurately tracing water movement (Ma and Song, 2016; Paces and Wurster, 2014).

Uneven precipitation distribution over the summer maize and winter wheat seasons in the NCP makes crop water uptake patterns highly temporal heterogeneity (Chesson et al., 2004; Moreno-Gutierrez et al., 2012). To identify the water source and water uptake layers, soil layer classification is the primary issue need to be addressed. Currently, there are four main ways to address classifying the water source. Firstly, some studies provided no clear explanations for soil layers classification, such as those of Wang et al. (2010), Zhang et al. (2011), Moreno-Gutierrez et al. (2012), David et al. (2013), Meissner et al. (2014), Wu et al. (2016), and Evaristo et al. (2016). Secondly, others (Ma and Song, 2016) classify soil layers based on the differences in the isotopic composition of soil water. In this case, soil was roughly sorted into shallow, middle, and deep soil layers that were respectively characterized by significant isotopic depletion, light isotopic depletion, and relatively isotopic stability. However, the isotopic compositions reflecting the soil layers characteristic were abstracted from other studies instead of real value in the study. In spite of applying local isotopic compositions of soil layers for soil classification, this also lacks of a statistical analysis of the isotopic composition as in Dai et al. (2015), Song et al. (2016), and Wu et al. (2014). Thirdly, others considered that the root distribution could be used to classify soil layers (Ma and Song, 2016). However, this requires determining the root density in each soil layer prior to the study, which is costly and time- and labor-intensive, especially for plants having long roots in the desert (Dai et al., 2015; Wu et al., 2014). As a matter of fact, soil water content is considered as an environmental factor and resource supply that affects crops. It is easy to be measured and could be a good index for soil classification (Ma and Song, 2016). However, there are few reports on this especially based on statistical analysis.

Although increasing attention has been paid to plant water uptake using stable isotopes in different ecosystems, such as forests (David et al., 2013; Evaristo et al., 2016; Li et al., 2007; Meissner et al., 2014; Moreno-Gutierrez et al., 2012; Song et al., 2016; Yang et al., 2015), croplands (Ma and Song, 2016; Wang et al., 2010; Wu et al., 2016; Zhang et al., 2011), and deserts (Dai et al., 2015; Wu et al., 2014), this issue is far from being fully understood. In a cropland ecosystem, former studies emphasized only one type of crop (Ma and Song, 2016; Zhang et al., 2011). For studies that investigated several plants, the main focus was on co-existing plants spatially competing or cooperating for water resources (Meissner et al., 2014; Moreno-Gutierrez et al., 2012; Wu et al., 2014; Yang et al., 2015). However, studies on winter wheat and summer maize's use of water resources when planted sequentially in a crop rotation are lacking. Furthermore, crop water uptake varies with growth stages; however, previous studies mainly focused on a few growth stages, which may neglect accurate water-sensitive or water-extensive consumption growth stage. For example, Wang et al. (2010) and Zhang et al. (2011) indicated that the shifting water uptake layer lies in the flowering and full ripe stages for summer maize and in the milking and heading stages for winter wheat, but neglected the intervening growth stages. This relatively large temporal scale could not result in precise recommendations for irrigation practices.

To remedy this deficiency, stable isotopes δ^{18}O and δ^{2}H were applied to quantify water uptake in a summer maize and winter wheat rotation field in the NCP. The specific objectives of this study are: 1) to identify the main water uptake layers of summer maize and winter wheat at full growth stages; 2) to calculate the contributions of water uptake from each water source at different growth stages for summer maize and winter wheat; 3) to explore the relationships between crop water uptake and relevant factors; and 4) to optimize current irrigation management practices.

2. Materials and methods

2.1. Site description

This study was conducted at the Yucheng Comprehensive Experiment Station (YCES), Chinese Academy of Sciences, which is located in Dezhou (36°56′N, 116°40′E, 23 m a.s.l.), NCP. It has a warm temperate semi-humid and semi-arid climate. The annual mean air temperature is 13.3 °C and the annual precipitation is 559.8 mm according to the long-term observation in YCES (1980–2015). Precipitation is distributed unevenly, with 70% of the annual precipitation falling between June and September. The annual sunshine is 2640 h. The soil type is Aquents with high salinity (Soil Survey Staff, 1999). A winter wheat–summer maize rotational cropping system predominates at this study site.

2.2. Sample collection

The sampling campaigns were carried out in the Sino-Japanese Joint Field at the YCES from June 2015 to July 2016. The field was rotationally planted with wheat (*Triticum aestivum* L., Jimai-22) and maize (*Zea mays* L., HY-1). Wheat and maize were sown in mid-October and mid-June, respectively, and harvested in early June and early October, respectively. Fertilizer was generally applied at the following three times: 1) before wheat sowing, 2) in March, and 3) between the jointing and flare opening stage of maize. Also, irrigation sessions were carried out at the following three times: 1) in March, 2) between the booting and flowering stages of wheat, and 3) before maize sowing.

Crop xylem, soil, and root samples at different depths were collected at eight growth stages from winter wheat (wintering, seedling, jointing, booting, heading, flowering, milking, and mature stages) and summer maize (trefoil, jointing, booting, heading, silking, milking, mature, and harvest stages). Also, soil at different depths after a precipitation event was collected. Xylem was cut from crops and the epidermis was gently removed using tweezers. Accordingly, roots at 0–5, 5–10, 10–20, 20–40, 40–60, 60–80, and 80–100 cm soil layers were extracted using a soil auger (10-cm diameter) with a sharpened edge. Adjacent soil samples were collected at layers of 0–5, 5–10, 10–20, 20–40, 40–60, 60–80, 80–100, 100–120, 120–150, and 150–200 cm using a 10-cm diameter auger. Then, the xylem and soil samples were quickly placed into 20-

ml screw-cap glass vials sealed with Parafilm and stored in a refrigerator at −4 °C until extraction.

Samples were collected after precipitation into 100-ml polyethylene air-tight vials using a funnel with a ping-pang ball (Li et al., 2007).

2.3. Measurement and analysis

Soil water content at depths of 10 cm, 20 cm, 30 cm, 40 cm, 60 cm, 80 cm, 100 cm, 120 cm, 150 cm, and 200 cm were monitored at 30 min intervals using a Water-Content-Profile probe (EnviroSCAN, Sentek Pty Ltd., Stepney, Australia) connected to a CR200X data logger (Campbell Scientific, Inc. Logan, UT, USA) in the field.

Water in xylem and soil samples were extracted using a fully automatic vacuum condensation extraction system (LI-2100, LICA United Technology Limited, Beijing, China). The extraction rate of water from samples was >98%. Xylem water, soil water, and precipitation (0.5–1.5 ml) (manual book edited by Los Gatos Research, Inc.) were analyzed for $\delta^{18}O$ and $\delta^{2}H$. The isotopic compositions were analyzed using a water isotope analyzer (WIA-35d-EP, Model 912-0026, Los Gatos Research, Mountain View, CA, USA). Each sample was analyzed six times, and the first three results were discarded to minimize the memory effect. The isotopic compositions were reported in standard δ-notation, representing ‰ deviations from the Vienna Standard Mean Ocean Water standard (V-SMOW), expressed as $\delta(‰) = \frac{R_{sample} - R_{standard}}{R_{standard}} \times 1000 = (\frac{R_{sample}}{R_{standard}} - 1) \times 1000$. The analytical uncertainties for $\delta^{18}O$ and $\delta^{2}H$ were 0.15‰ and 0.5‰, respectively. Corrections using a standard curve for $\delta^{18}O$ and $\delta^{2}H$ in xylem water samples were conducted to avoid methanol and ethanol contamination (Schultz et al., 2011).

Roots were washed, sieved, and then oven-dried at 65 °C to a constant weight to achieve dry root weights. The dry root weight density was calculated by dividing the dry root weight (g) by the soil volume (cm^3) (Guan et al., 2015; Li et al., 2010).

The Bayesian mixing model (MixSIR 1.0.4) was employed to quantify the proportion of water uptake from each water source based on the mass balance of the isotope (Moore and Semmens, 2008).

2.4. Statistical analyses

A hierarchical cluster analysis (HCA) was used to classify the soil layers according to the similarities of the soil volumetric water contents between the soil depths. Before data standardization by z-score normalization, Ward's method, based on Euclidean distance, was chosen for classification. A one-way analysis of variance with Duncan's post-hoc test ($p \leq 0.05$) was conducted to test for significant differences in $\delta^{18}O$ and $\delta^{2}H$ at different soil layers and between the summer maize and winter wheat seasons at each soil layer. Prior to analysis, all of the variables were checked for distribution normality (Shapiro–Wilk test) and homogeneity (Levene test). All statistical analyses were performed using SPSS software (SPSS Inc., Chicago, IL, USA).

3. Results

3.1. Meteorological condition

Variations in precipitation, air temperature, and accumulated precipitation during the whole growth seasons of winter wheat and summer maize are shown in Fig. 1. The total precipitation throughout the experimental period was 422.0 mm, 292.0 mm of which fell in the summer maize season, while the remaining of 131.0 mm fell in the winter wheat season (Fig. 1b). The mean air temperature differed greatly between the summer maize (24.0 °C) and winter wheat (7.9 °C) seasons. The mean air temperature over the both growth seasons was 13.2 °C. Heavy precipitation and high air temperature occurred simultaneously in the summer maize season, while the winter wheat season had less precipitation and lower air temperature.

3.2. Soil volumetric water content and HCA

The soil volumetric water content was characterized by stratification during the experimental period (Fig. 2). The mean soil volumetric water content (mean ± standard deviation) at 10 cm, 20 cm, 30 cm, 40 cm, 60 cm, 80 cm, 100 cm, 120 cm, 150 cm, and 200 cm are showed in Fig. 2. The soil volumetric water content increased with soil depth, then decreased, being the greatest at 150 cm and the lowest at 10 cm.

A more specific classification of soil layers was possible based on the HCA of soil volumetric water content shown in Fig. 3. The 10 soil depths were first classified into two groups, Group I and Group II. Group I included 10 cm, 20 cm, 30 cm, and 40 cm. While 60 cm, 80 cm, 100 cm, 120 cm, 150 cm, and 200 cm fell into Group II. Then two subgroups were derived from each Group. For Group I, Subgroup I contained 20 cm, while other three soil depths were classified as Subgroup II. Similarly, Subgroup I of Group II contained 200 cm. Subgroup II of Group II contained the other five soil depths. In practice, 10 cm has closely

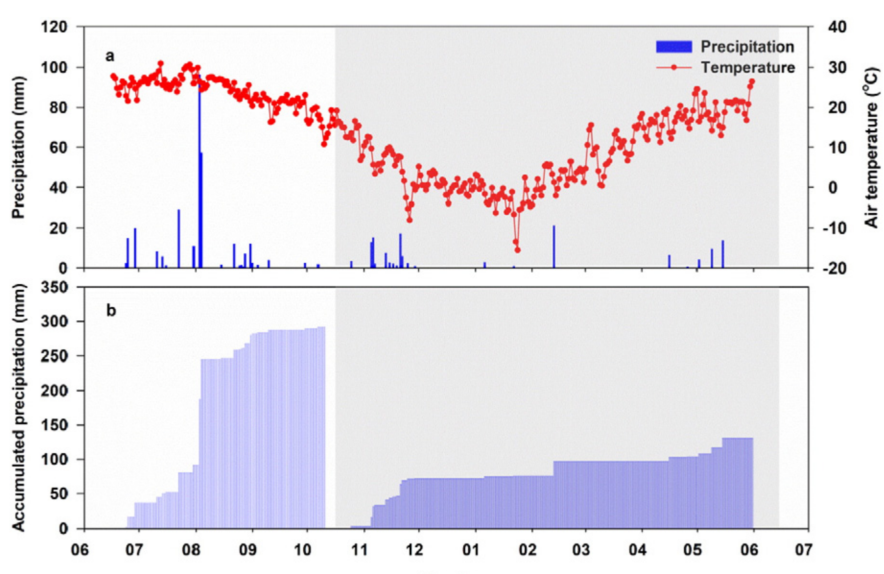

Fig. 1. Daily precipitation and air temperature (a), accumulated precipitation (b) during the experimental period. The white area indicates the summer maize season, and the grey area indicates the winter wheat season.

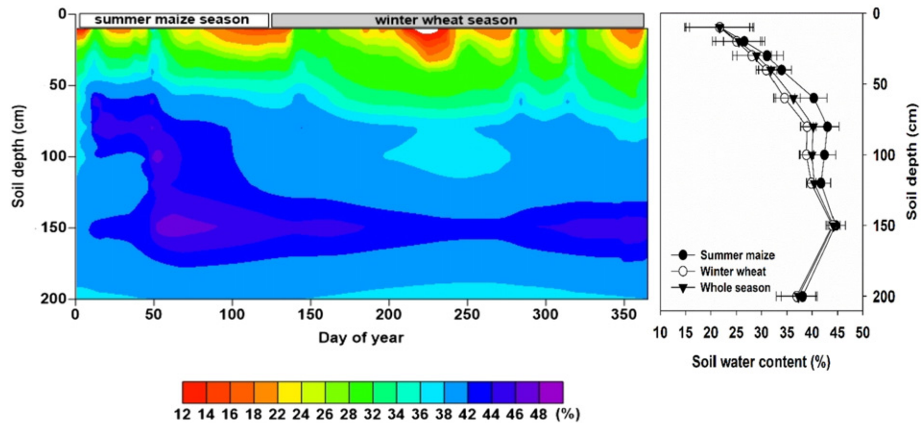

Fig. 2. Daily soil volumetric water content (SVWC) during the experimental period. Different colors represent different soil volumetric water content. Mean soil water content at each soil depth during the summer maize season, winter wheat season, and whole season are depicted on the right-side. Bars denote standard deviation.

spatially connected with 20 cm but not 30 cm or 40 cm. Similarly, 150 cm was more closely connected with 200 cm than with 60 cm or the other three depths (80 cm, 100 cm, 120 cm). Finally, the four parts were rearranged as follows: 1) 10 cm and 20 cm; 2) 30 cm and 40 cm; 3) 60 cm, 80 cm, 100 cm, and 120 cm; 4) 150 cm and 200 cm.

3.3. Isotopic composition of precipitation, xylem water, and soil water

The δ^{18}O and δ^2H of precipitation during the experimental period showed a broad range from −10.09 to −2.77‰ and −80.6 to −9.5‰, with mean values of −5.93‰ and −39.4‰, respectively (Table 1). The local meteoric water line (LMWL) was obtained from local precipitation samples and could be expressed as $\delta^2H = 7.04 \times \delta^{18}O + 2.29, R^2 = 0.79, p < 0.01$ (Fig. 4). The slope, 7.04, was lower than the slope of 8, which was derived from the global meteoric water line (GMWL) $\delta^2H = 8 \times \delta^{18}O + 10$ (Craig, 1961).

The isotopic composition of xylem water varied slightly during the experimental period (Fig. 5). The mean δ^{18}O and δ^2H values of xylem water were −7.56‰ and −65.4‰, respectively, for summer maize, and −7.12‰ and −58.8‰, respectively, for winter wheat (Table 1). The δ^2H–δ^{18}O relationship in xylem water could be expressed as $\delta^2H = 4.49 \times \delta^{18}O - 29.13, R^2 = 0.68, p < 0.01$ (Fig. 4), which was called the xylem water line (XWL). The XWL for summer maize and winter wheat were $\delta^2H = 2.95 \times \delta^{18}O - 43.09, R^2 = 0.82, p < 0.01$ and $\delta^2H = 5.52 \times \delta^{18}O - 19.46, R^2 = 0.91, p < 0.01$, respectively.

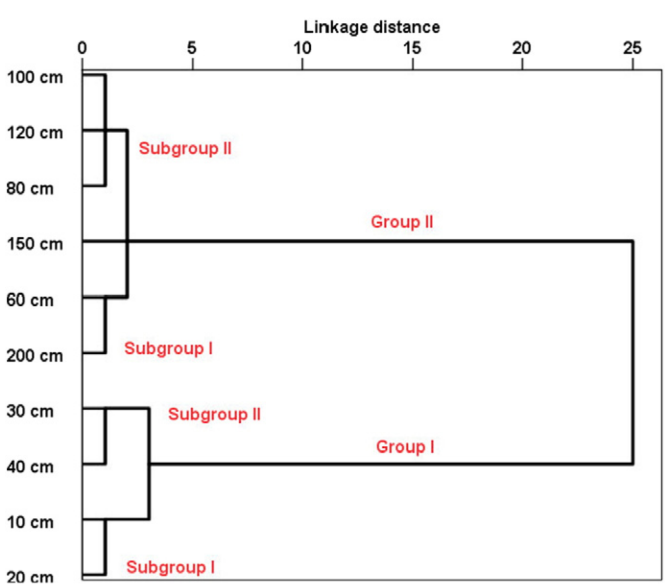

Fig. 3. Dendrogram of the hierarchical cluster analysis of the soil volumetric water content.

The δ^{18}O and δ^2H values of soil water at 11 soil depths are list in Table 1. For summer maize, The mean δ^{18}O and δ^2H values of soil water were −8.14‰ and −65.9‰, with the highest values of −2.46‰ (5 cm) and −36.5‰ (10 cm), respectively, and lowest values of −11.15‰ (20 cm) and −78.0‰ (10 cm), respectively. For winter wheat, the mean δ^{18}O and δ^2H values of the soil water were −7.89‰ and −62.7%, respectively. The respective highest and lowest isotopic compositions occurred at 5 cm and 100 cm.

Based on the results of HCA, the variations in the isotopic composition of the soil water were divided into four groups, as shown in Fig. 5. The δ^{18}O and δ^2H values of the soil water at the 0–20 cm layer were both significantly higher than that at the other three soil layers ($p < 0.01$), whereas the δ^{18}O and δ^2H values of the soil water at 20–40 cm, 40–120 cm, and 120–200 cm did not differ significantly ($p > 0.05$). As for the effect of the crops, there was no significant difference ($p > 0.05$) in δ^{18}O and δ^2H values between the summer maize season and winter wheat season at of the 0–20 cm and 20–40 cm layers, but there were at the 40–120 cm and 120–200 cm ($p < 0.05$) layers.

The soil water line (SWL), $\delta^2H = 5.32 \times \delta^{18}O - 21.33, R^2 = 0.81, p < 0.01$, obtained from the soil water samples in this study, is plotted in Supplementary Information (Fig. S1). The SWLs for summer maize and winter wheat were $\delta^2H = 4.54 \times \delta^{18}O - 28.73, R^2 = 0.84, p < 0.01$ and $\delta^2H = 5.59 \times \delta^{18}O - 18.63, R^2 = 0.81, p < 0.01$, respectively. SWLs changed with the soil layer (Fig. S1). During the summer maize season, the SWLs at 0–20 cm, 20–40 cm, 40–120 cm, and 120–200 cm were $\delta^2H = 4.92 \times \delta^{18}O - 26.86, R^2 = 0.91, p < 0.01$, $\delta^2H = 5.06 \times \delta^{18}O - 24.64, R^2 = 0.79, p < 0.01$, $\delta^2H = 3.62 \times \delta^{18}O - 36.56, R^2 = 0.76, p < 0.01$, and $\delta^2H = 3.90 \times \delta^{18}O - 32.34, R^2 = 0.90, p < 0.01$, respectively. During the winter wheat season, the SWLs at 0–20 cm, 20–40 cm, 40–120 cm, and 120–200 cm were $\delta^2H = 4.73 \times \delta^{18}O - 22.72, R^2 = 0.69, p < 0.01$, $\delta^2H = 5.04 \times \delta^{18}O - 24.72, R^2 = 0.71, p < 0.01$, $\delta^2H = 4.26 \times \delta^{18}O - 30.46, R^2 = 0.61, p < 0.01$, and $\delta^2H = 3.48 \times \delta^{18}O - 35.83, R^2 = 0.27, p < 0.01$, respectively.

3.4. Variations of isotopic composition in xylem water and soil water at distinct soil layers

The comparisons of δ^{18}O and δ^2H values between xylem water and soil layer water at growth stages during the summer maize and winter wheat seasons are plotted in Fig. 6. Based on the assumption that no isotope fractionation occurred during root water uptake and plant water transport in most plants (Dawson and Ehleringer, 1991; Ehleringer and Dawson, 1992; Zimmermann et al., 1967), xylem can be regarded as the mixture of several water sources. Therefore, it is feasible to

Table 1
General characteristics of the isotopic composition in precipitation, soil water and xylem water samples across all sampling times.

Season	Sample type	Soil depth (cm)	N	$\delta^{18}O$ (‰)				δ^2H (‰)			
				Max.	Min.	Avg.	SD	Max.	Min.	Avg.	SD
Summer maize	Soil water	5	15	−2.46	−9.98	−6.26	2.32	−45.0	−74.8	−59.3	9.67
		10	15	−5.78	−11.11	−7.93	1.66	−36.5	−78.0	−65.7	10.25
		20	13	−7.23	−11.15	−8.96	0.95	−59.7	−77.2	−69.6	4.45
		30	14	−6.10	−9.98	−8.67	1.09	−59.7	−77.2	−69.3	4.52
		40	14	−6.85	−9.92	−8.61	0.75	−46.1	−72.5	−67.3	6.48
		60	15	−6.88	−9.36	−8.30	0.85	−63.2	−73.6	−67.4	3.65
		80	15	−6.13	−9.49	−8.07	0.84	−60.5	−69.7	−65.7	3.00
		100	15	−6.62	−9.73	−8.24	0.85	−60.6	−73.8	−66.2	3.75
		120	15	−7.27	−9.69	−8.34	0.74	−60.7	−72.0	−65.9	3.25
		150	14	−6.63	−9.97	−8.31	0.89	−54.9	−70.0	−64.6	4.16
		200	15	−4.58	−9.16	−8.04	1.20	−53.3	−67.6	−63.9	3.71
		Total	160	−2.46	−11.15	−8.14	1.34	−36.5	−78.0	−65.9	6.16
	Xylem water		8	−6.35	−9.68	−7.56	1.13	−60.2	−71.0	−65.4	3.66
Winter wheat	Soil water	5	29	−1.02	−9.64	−5.27	2.57	−17.5	−65.4	−44.7	13.80
		10	28	−3.65	−9.12	−6.86	1.66	−33.1	−71.7	−55.1	10.23
		20	29	−6.23	−9.20	−7.87	0.72	−52.2	−72.4	−63.5	5.74
		30	29	−6.22	−9.07	−8.05	0.66	−56.2	−72.0	−65.0	3.76
		40	30	−7.32	−9.16	−8.28	0.44	−59.8	−71.6	−66.7	2.64
		60	30	−7.28	−9.13	−8.36	0.43	−61.5	−72.4	−66.9	2.40
		80	30	−7.53	−9.10	−8.36	0.37	−61.2	−70.7	−66.0	1.92
		100	30	−7.04	−9.75	−8.47	0.49	−60.4	−72.7	−66.3	2.34
		120	29	−6.59	−9.09	−8.26	0.54	−55.5	−69.4	−64.9	2.97
		150	30	−7.70	−9.06	−8.41	0.33	−61.7	−72.2	−65.4	2.36
		200	28	−7.82	−9.53	−8.52	0.37	−60. 5	−70.2	−65.0	2.42
		Total	322	−1.02	−9.75	−7.89	1.37	−17.5	−72.7	−62.7	8.67
	Xylem water		8	−5.97	−8.41	−7.12	0.89	−52.3	−66.5	−58.8	5.15
	Precipitation		17	−2.77	−10.09	−5.93	2.41	−9.5	−80.6	−39.4	19.02

determine the main water source for crop growth by comparing the isotopic composition of xylem water and source water. Thus, the intersection of the isotopic composition of xylem water and soil water indicates the main water uptake source (Wang et al., 2010; Yang et al., 2015).

For summer maize, the $\delta^{18}O$ of xylem water interacted with the soil layer of 5–10 cm at the trefoil stage, 10–20 cm at the jointing stage, 30–40 cm and 100–120 cm at the booting stage, 40 cm at the heading stage, 40–60 cm and 150–200 cm at the silking stage, 10–20 cm and 80–120 cm at the mature stage, and 10 cm and 80 cm at the harvest stage. The δ^2H of xylem water interacted with the soil layer of 5–10 cm at the trefoil stage, 10–15 cm at the jointing stage, 30–40 cm at the booting stage, 20–40 cm and 60–80 cm at the heading stage, 5–10 cm and 40–60 cm at the silking stage, and 10–15 cm and 80–100 cm at the mature stage. At the milking stage, more than two interactions were found.

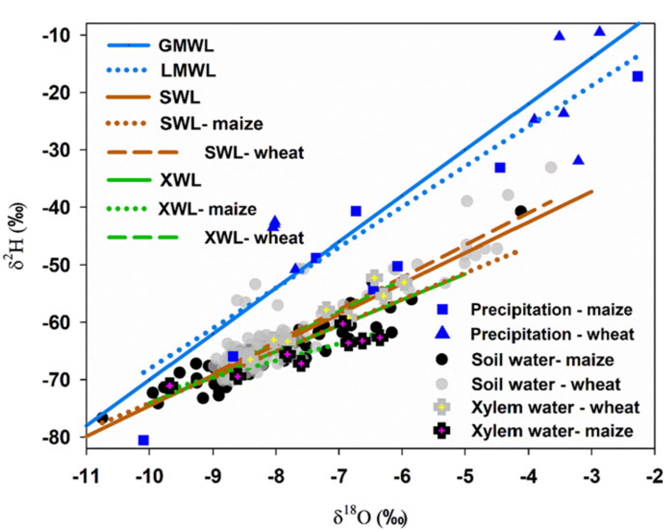

Fig. 4. δ^2H–$\delta^{18}O$ relationships in precipitation, soil water, and xylem water during the summer maize and winter wheat seasons. The blue solid square and blue solid triangle denote precipitation of summer maize and winter wheat, respectively. The black and grey solid circles denote the soil water of summer maize and winter wheat, respectively. The black and grey crosses denote the xylem water of summer maize and winter wheat, respectively. The blue solid line, blue dotted line, brown solid line, and green solid line represent the global meteoric water line (GMWL), local meteoric water line (LMWL), soil water line (SWL), and xylem water line (XWL), respectively. The brown dotted line and brown dash line denote the SWLs of summer maize and winter wheat. The green dotted line and green dash line denote XWLs of summer maize and winter wheat.

For winter wheat, the $\delta^{18}O$ of xylem water interacted with the soil layer of 5–10 cm at the wintering stage, 10 cm at the seedling stage, 18 cm at the jointing stage, 30 cm at the booting stage, 10–20 cm at the milking stage, and 18–19 cm at the mature stage. The δ^2H of xylem water interacted with the soil layer of 5–10 cm and 20–30 cm at the wintering stage, 12 cm at the seedling stage, 17 cm at the jointing stage, 10–20 cm at the booting stage, 10–20 cm at the milking stage, and 10–20 cm at the mature stage. There were more than two interactions during the heading and flowering stages.

3.5. Contribution of each water source to crop water uptake

The contribution of each soil layer water for crop use changed over the growth stages for summer maize and winter wheat (Fig. 7). For summer maize, 77.8 ± 1.6% and 48.6 ± 2.7% of water for crop use was from the 0–20 cm soil layer at the trefoil and jointing stages. At the booting and heading stages, the water uptake proportions were 33.6 ± 24.5% and 32.6 ± 23.3%, respectively, at 20–40 cm. The main water uptake layer changed to 40–120 cm at the silking and milking stages with proportions of 32.0 ± 4.3% and 36.7 ± 21.9%, respectively. From the mature to harvest stages, summer maize mainly absorbed water at shallow soil layers (0–20 cm) again, and the proportion also showed an increasing trend, from 35.0 ± 4.7% to 52.4 ± 2.1%. Winter wheat had relatively simple variations in water uptake based on soil depth. The major soil layer was 0–20 cm at the wintering (86.6 ± 1.0%), seedling (83.7 ± 1.7%), jointing (45.2 ± 1.3%), booting (51.4 ± 4.4%), heading (28.8 ± 17.8%), and mature (67.8 ± 0.6%) stages. At the flowering and milking stages, the main water uptake layer changed to

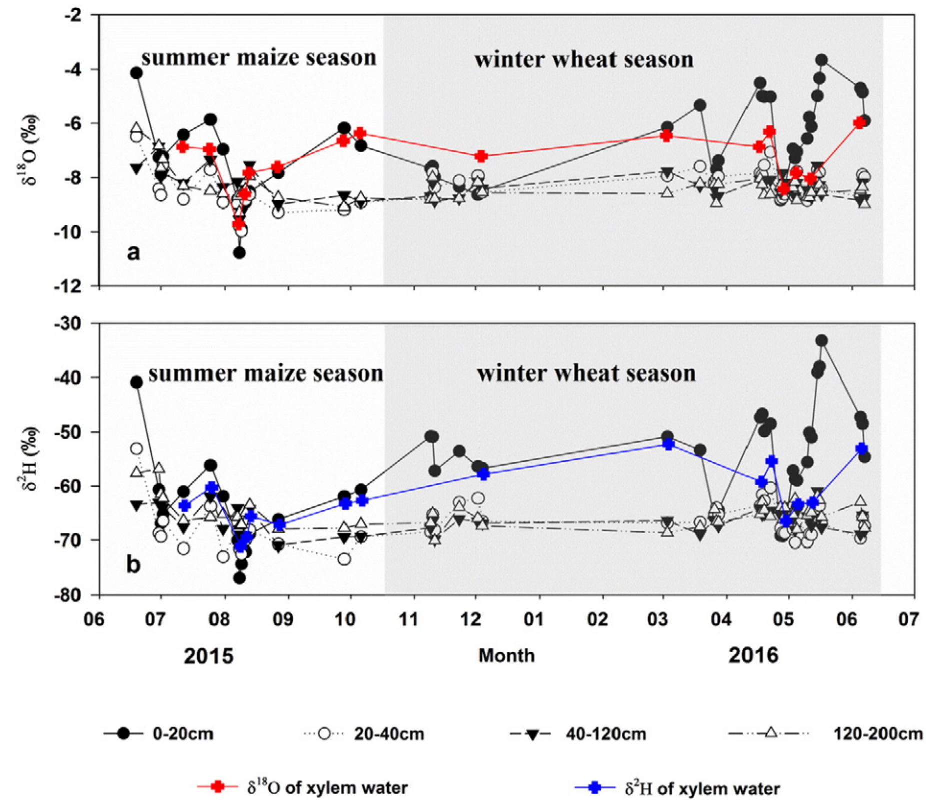

Fig. 5. Temporal variations in $\delta^{18}O$ (a) and $\delta^{2}H$ (b) in soil water and xylem water from June 2015 to July 2016. The white area indicates the summer maize season, and the grey area indicates the winter wheat season.

20–40 cm, with proportions of 34.8 ± 24.9% and 25.2 ± 17.0%, respectively.

4. Discussion

4.1. Soil layer classifications and soil depth sampling

Classifying the water source is necessary before determining plant water uptake. The soil water content should be considered when making soil layer classification, but it has been often ignored in previous studies (David et al., 2013; Evaristo et al., 2016; Meissner et al., 2014; Moreno-Gutierrez et al., 2012; Wang et al., 2010; Wu et al., 2016; Zhang et al., 2011). To make up for the shortcomings mentioned in the introduction, this study jointly considered isotopic differences in the soil water and the soil water content using an HCA for soil classification. The isotopic composition of soil water at the 0–20 cm layer was significantly greater than that at the other soil layers ($p < 0.01$), which did not differ significantly ($p > 0.05$) among themselves. Based on this result, the 0–20 cm soil layer was distinguished from all of the soil layers. Thus, the soil water content was considered to classify soil layers. As an effective statistical analysis, HCA classifies variables to specific groups based on their similarity levels (Wang et al., 2014). This not only reduces the number of variables, but also emphasizes the heterogeneity between the groups. The soil water content, as an indicator for soil layer classifications, has advantage, such as being easily obtained, allowing frequent monitoring, and having a small error, that other indicators could not match. Based on the HCA on the soil volumetric water content, in combination with the results of the soil water isotopic composition, soil layers were consequently divided into four groups: 0–20 cm, 20–40 cm, 40–120 cm, and 120–200 cm.

The sampling depth of the soil layers depends on the ecosystem type. Studies on plant water uptake using stable isotopes, as shown in Fig. S2 in Supplementary Information, demonstrated that sampling soil depths were no >100 cm in forests, reached 300 cm in deserts, and were between 100 cm and 200 cm in croplands. This can be explained by the root distribution. In deserts, plants have long roots, and even a 300 cm soil depth did not include the whole root system (Dai et al., 2015). This is generally resolved by collecting groundwater adjacent to the soil samples (Dai et al., 2015). It is difficult to determine the soil sampling depths based on root distributions for plants in forests, which are affected by variations in topography. Crops root-length characteristics are considered when determining sampling soil depth. For most crops, scarcely any roots were found below 120 cm, and 200 cm is commonly regarded as the critical depth when studying the soil–groundwater interface (Zhang et al., 2004; Xue et al., 2003). Thus, the sampling depth for used in this study of cropland soil layers is reasonable.

4.2. Comparison of crop water uptake and its potential mechanisms

Contributions of different soil layers to water uptake for summer maize and winter wheat changed over the growth stages (Fig. 7). This is associated with the variations in crop water requirements at different growth stages. Although different proportions of water uptake came from different soil layers, summer maize and winter wheat both showed a similar trend in which they firstly predominately absorbed shallow soil water, then deep soil water, consequently returned to shallow soil water. This result is consistent with previous studies in croplands (Ma and Song, 2016; Wang et al., 2010; Zhang et al., 2011). The main soil layer of water uptake extends to deeper soil layer at different growth stages, occurring in the booting stage for summer maize and in the flowering stage for winter wheat. During the booting stage, summer maize requires much water for vegetative and reproductive growth. In contrast to winter wheat, summer maize continually absorbed water from a much deeper soil layer. From the silking to milking stages, the major layer of water uptake was 40–120 cm because of the great water demand during these growth stages. Winter wheat mainly absorbed shallow (0–20 cm) soil water during most growth stages,

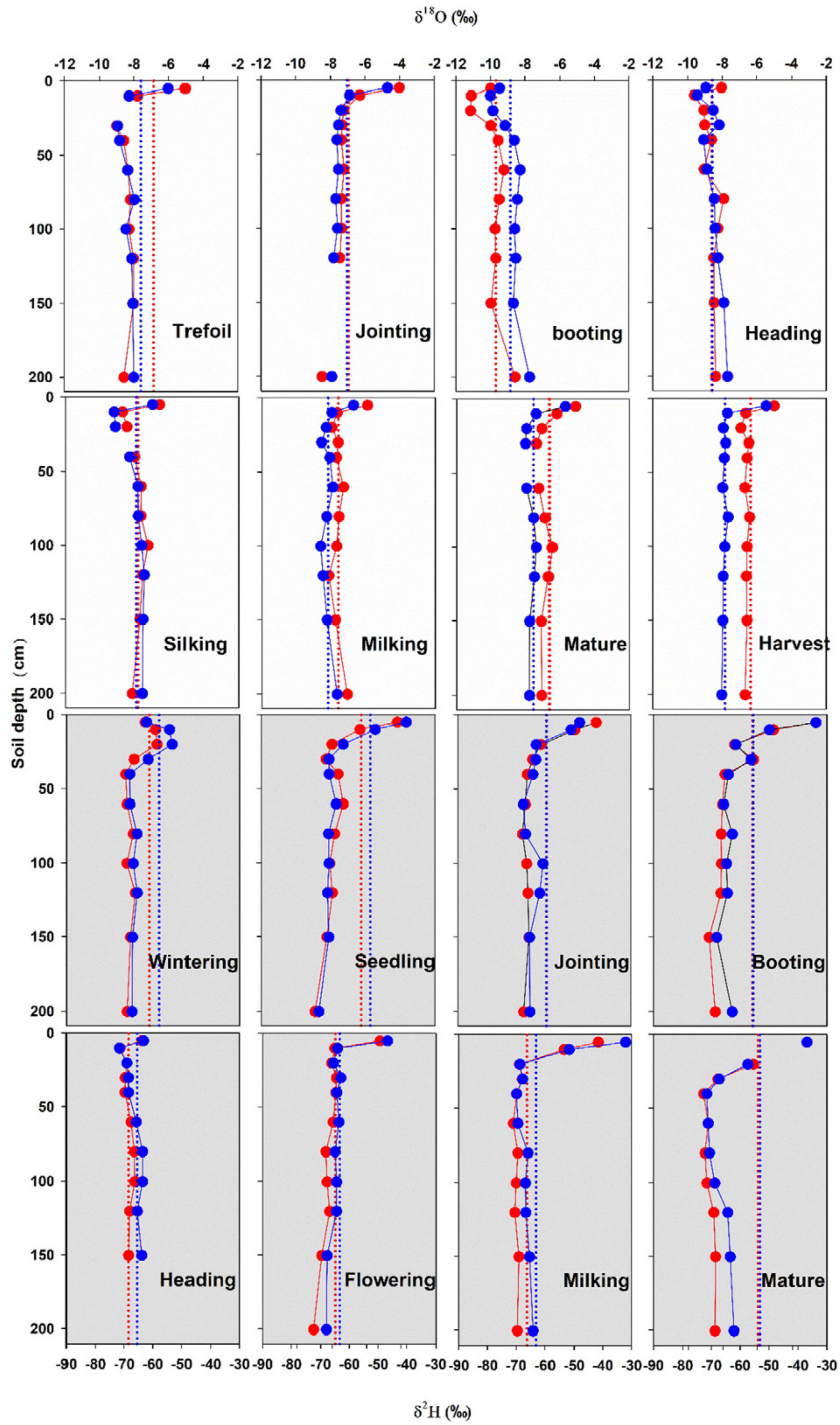

Fig. 6. $\delta^{18}O$ and $\delta^{2}H$ in soil layers (0–200 cm) and xylem water at different growth stages of summer maize (white area) and winter wheat (grey area). Red symbols and blue symbols denote $\delta^{18}O$ and $\delta^{2}H$, respectively. Red and blue dotted lines indicate $\delta^{18}O$ and $\delta^{2}H$ in xylem water, respectively. Note: breakpoints indicate that $\delta^{18}O$ and $\delta^{2}H$ were not detected at certain soil depths.

except it absorbed from 20–40 cm during the flowering and milking stages. Water was needed to meet the greatest water uptake requirement for reproductive growth in the flowering stage and for grain weight increase in the milking stage (Fang et al., 2010; Li et al., 2005). As the crops entered the mature stage, the water demand required for both crops decreased due to shrinking roots.

The shifting main water uptake layer during growth stage may be explained by root system development. Summer maize and winter

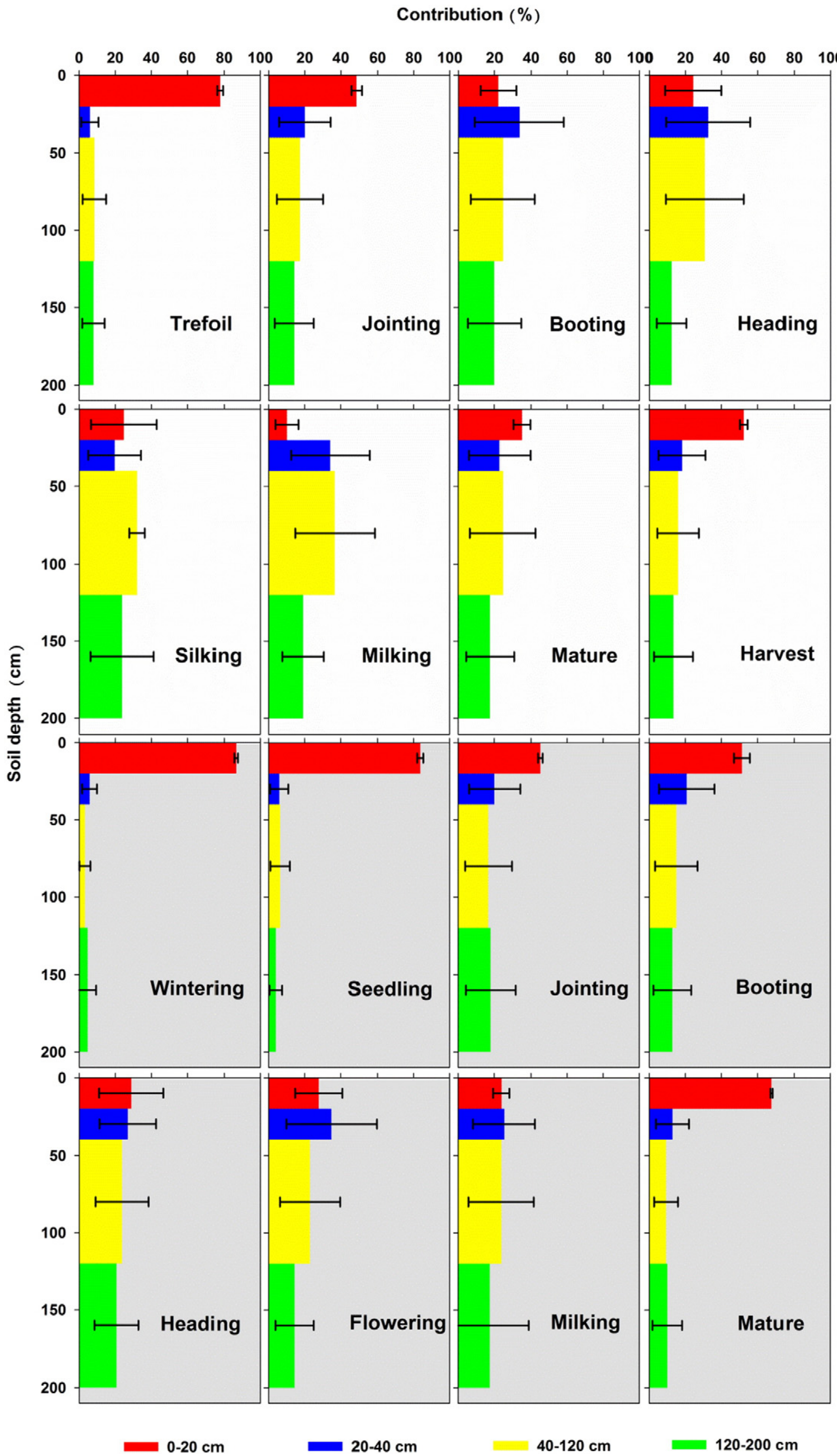

Contribution（%）
0
20
40
60
80
100
Soil depth（cm）
0
50
100
150
200
Trefoil
Jointing
Booting
Heading
Silking
Milking
Mature
Harvest
Wintering
Seedling
Jointing
Booting
Heading
Flowering
Milking
Mature
0-20 cm
20-40 cm
40-120 cm
120-200 cm

wheat both have fibrous root systems, which consist of seminal and nodal roots, with the majority of the roots developing at 0–40 cm (Aggarwal et al., 2006; Li et al., 2006). In this study, dry root weight density, as an indicator of crop water uptake, was chosen for analysis (Aina and Fapohunda, 1986; Li et al., 2006). Fig. 8 showed that 97.4% and 89.2% of the dry root weight was distributed in 0–10 cm and 0–40 cm soil layers for summer maize and winter wheat, respectively. This was within the range described by previous studies in croplands (Fig. S2). Further evidence indicated that the dry root weight density of winter wheat was positively correlated with the contribution of water uptake ($r = 0.72$, $p < 0.01$), suggesting that root distribution positively responded to the winter wheat water uptake. However, no similar correlation was found in summer maize (Fig. 8). This did not mean that the summer maize root system's development could not explain water uptake. Unlike in winter wheat, aboveground aerial roots in summer maize support crop growth and account for a large percentage of the shallow root weight. Additionally, maize roots extend to deeper soil, and these roots may be more efficient in absorbing deep soil water (Li et al., 2006; Camposeo and Rubino, 2003; Draye et al., 2010). However, using root distribution as an indicator has been questioned, because it may not reflect actual water uptake temporal and spatial variations (Ehleringer and Dawson, 1992), which depend on root activity (Donovan and Ehleringer, 1994; Wu et al., 2014).

Because of small differences in the isotopic composition of soil water in the soil profile at some growth stages (such as the milking and harvest stages of summer maize, and the heading and flowering stages of winter wheat), determining the water uptake layer by direct comparison is not powerful. The soil water content consequently can be taken into consideration when determining the water uptake (Wang et al., 2010; Yang et al., 2015). The soil volumetric water content in the summer maize season differed from that of the winter wheat season (Fig. 2), having mean values of 36.4% and 34.0%, respectively. A regression analysis indicated that the contribution of water uptake (CWU) was negatively correlated with the soil volumetric water content (SVWC). Thus, $CWU = -0.91 \times SVWC + 57.75, r = 0.48, p = 0.0052, n = 32$ and $CWU = -2.03 \times SVWC + 92.73, r = 0.66, p < 0.0001, n = 32$ were finally obtained for summer maize and winter wheat, implying that crop water uptake could result in soil drying. Soil layers were classified based on soil volumetric water contents, which corresponded to the contributions of crop water uptake. This correlation for summer maize was less than for winter wheat. Summer maize and winter wheat experienced frequent precipitation events and water-limited conditions, respectively (Figs. 1 and 2). The summer maize season coincided with the rainy season in which the frequent precipitation events facilitated moistening the soil (Fig. 2). The extent of precipitation recharges soil water depends on the amount. Thus, small precipitation events recharge shallow soil water, while heavy precipitation events recharge deep soil water (Wu et al., 2014). Winter wheat was constrained by water deficits, especially from the wintering to seedling stages (Fig. 2), and the low water availability affected the following period of water uptake (Yang et al., 2015). The time lag effect of the water deficit exerted its influence on water uptake several days later (Tang et al., 2014). Hydraulic redistribution, which commonly occurs during dry conditions, sustains crop water uptake by roots that passively transport soil water along a hydraulic gradient (Richards and Caldwell, 1987; Sprenger et al., 2016). Nevertheless, results from Walter (2010) showed that the influence of hydraulic redistribution on the isotopic composition of soil pore water is limited.

4.3. Instructions for current agricultural water management

The key goal for studying crop water uptake in croplands is to provide reasonable water management strategies, especially irrigation schemes. At present, free flooding irrigation is universal. However, this is a waste of water resources. Additionally, the rise in the groundwater table depth could lead to soil salinization or root growth inhibition caused by oxygen stress in soils, ultimately reducing grain yields (Liu et al., 2001; Zipper et al., 2015). Although summer maize and winter wheat both have water uptake patterns that alter their water sources from shallow to deeper soils, and then back to shallow soils, the variation in the main water uptake layers occurred during different growth stages, requiring different irrigation practices. In this study, summer maize and winter wheat absorbed water from deeper soils at the booting, silking, and mature stages, and at the flowering and milking stages, respectively. Summer maize season is grown during the rainy season. Therefore, expect for one irrigation time before maize sowing, no irrigation should be applied during the maize season because there is sufficient reserved soil water (Guan et al., 2015). Winter wheat grows during low water availability conditions because of the limited amount of precipitation, and thus requires frequent irrigation (Guan et al., 2015). As determined by Fang et al. (2010), a 4:1 irrigation water allocation between winter wheat and summer maize seasons at the NCP could achieve high grain yields and water use efficiency. At this study site, currently, two irrigation events occur in the winter wheat season, one in March and the other between the booting and flowering stages. The latter is earlier than required according to the dual stable isotope study, indicating that the current second irrigation could be suspended several days until the flowering stage, which demands the most water.

The amount of irrigation also deserves to be further investigated. Irrigation involves complex processes, including soil evaporation, precipitation infiltration, root water uptake, soil drainage, groundwater recharge, and their interactions. Thus, the amount of irrigation required

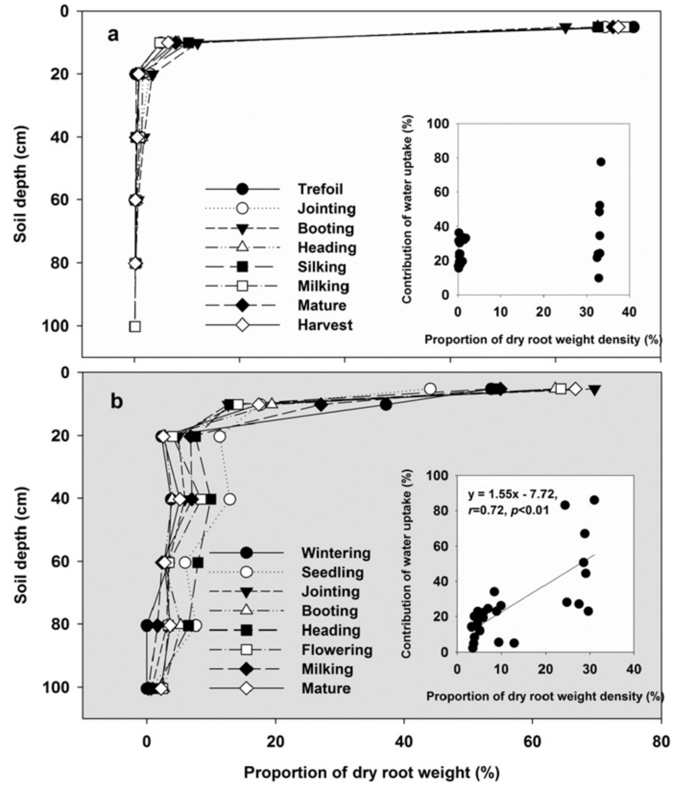

Fig. 8. Variations in the proportions of dry root weight density at different growth stages of summer maize (a) and winter wheat (b). The inset in each panel indicates the relationship between dry root density proportions and the water uptake contributions.

Fig. 7. Contribution of water uptake from 0–20 cm, 20–40 cm, 40–120 cm, and 120–200 cm soil layers at different growth sages of summer maize (white area) and winter wheat (grey area). Bars indicate standard deviation.

varies because of crops type, precipitation amount, soil type, and agronomic practices (Fang et al., 2010). Increasing the amount of irrigation might increase soil evaporation and decrease water use efficiency at the same time (Qiu et al., 2008). A study at the NCP by Zhang et al. (2011) showed that the irrigation wetting depth during winter wheat growth was reduced from the traditionally considered 100 cm to 40 cm. This indicated that routine irrigation regimes (three to five times) at the NCP results in over-irrigation and adversely affects grain yields (Qiu et al., 2008).

Although this study quantified the proportion of water uptake from different water sources at different growth stages, other related processes should be focused on in future studies. Furthermore, process-based modeling methods might be coupled with the stable isotopes method to improve the temporal resolution and to evaluate different irrigation practices under different scenarios.

5. Conclusions

Stable isotopes δ^{18}O and δ^{2}H were used to quantify the water uptake at different growth stages of summer maize and winter wheat. As the major water source, soil layers were classified into four groups, 0–20 cm, 20–40 cm, 40–120 cm, and 120–200 cm, based on an HCA of the soil volumetric water content. The main water uptake layer for summer maize and winter wheat changed during the growth stages from shallow to deeper soil, then to shallow soil again. However, variations in main water uptake layers occurred in different growth stages: booting (20–40 cm), silking (40–120 cm), and mature (0–20 cm) stages for summer maize, and flowering (20–40 cm) and mature (0–20 cm) stages for winter wheat. The root distribution and soil water content responded differently to water uptake. The dry root weight density was positively correlated with the water uptake contribution in winter wheat but not in summer maize. However, the soil volumetric water content was negatively correlated with the water uptake contribution in both summer maize and winter wheat. These different water uptake patterns and response mechanisms provide more accurate and locally adapted information regarding agricultural water practices. Here, one irrigation event should be postponed from the booting to flowering stage in the winter wheat season.

Conflict of interest statements

No conflict of interest exits in this manuscript, and the manuscript is approved by all authors for publication. On behalf of my co-authors, I would like to declare that the work described was an original research that has not been published previously, and not under consideration for publication elsewhere, in whole or in part.

Acknowledgments

We are sincerely thankful to Feifei Zhao, Guilian Pang, Shufang Wei for their help with field and laboratory assistance. This study was supported by the National Natural Science Foundation of China (41271047), the National Key Research and Development Program of China (2016YFD0800301), and the National Key Technology R&D Program of China (2012BAD05B0204).

Appendix A. Supplementary data

Supplementary data to this article can be found online at https://doi.org/10.1016/j.scitotenv.2017.10.315.

References

Aggarwal, P., Choudhary, K.K., Singh, A.K., Chakraborty, D., 2006. Variation in soil strength and rooting characteristics of wheat in relation to soil management. Geoderma 136, 353–363.
Aina, P.O., Fapohunda, H.O., 1986. Root distribution and water uptake patterns of maize cultivars field grown under differential irrigation. Plant Soil 94, 257–265.
Camposeo, S., Rubino, P., 2003. Effect of irrigation frequency on root water uptake in sugar beet. Plant Soil 253, 301–309.
Chesson, P., Gebauer, R.L.E., Schwinning, S., Huntly, N., Wiegand, K., Ernest, M.S.K., et al., 2004. Resource pulses, species interactions, and diversity maintenance in arid and semi-arid environments. Oecologia 141, 236–253.
Craig, H., 1961. Isotopic variations in meteoric waters. Science 133, 1702–1703.
Dai, Y., Zheng, X.J., Tang, L.S., Li, Y., 2015. Stable oxygen isotopes reveal distinct water use patterns of two *Haloxylon* species in the Gurbantonggut Desert. Plant Soil 389, 73–87.
David, T.S., Pinto, C.A., Nadezhdina, N., Kurz-Besson, C., Henriques, M.O., Quilho, T., et al., 2013. Root functioning, tree water use and hydraulic redistribution in *Quercus suber* trees: a modeling approach based on root sap flow. For. Ecol. Manag. 307, 136–146.
Dawson, T.E., Ehleringer, J.R., 1991. Streamside trees that do not use stream water. Nature 350, 335–337.
Donovan, L.A., Ehleringer, J.R., 1994. Water stress and use of summer precipitation in a great basin shrub community. Funct. Ecol. 8, 289–297.
Draye, X., Kim, Y., Lobet, G., Javaux, M., 2010. Model-assisted integration of physiological and environmental constraints affecting the dynamic and spatial patterns of root water uptake from soils. J. Exp. Bot. 61, 2145–2155.
Ehleringer, J.R., Dawson, T.E., 1992. Water uptake by plants-perspectives from stable isotope composition. Plant Cell Environ. 15, 1073–1082.
Evaristo, J., McDonnell, J.J., Scholl, M.A., Bruijnzeel, L.A., Chun, K.P., 2016. Insights into plant water uptake from xylem-water isotope measurements in two tropical catchments with contrasting moisture conditions. Hydrol. Process. 30, 3210–3227.
Fang, Q., Ma, L., Yu, Q., Ahuja, L.R., Malone, R.W., Hoogenboom, G., 2010. Irrigation strategies to improve the water use efficiency of wheat-maize double cropping systems in North China Plain. Agric. Water Manag. 97, 1165–1174.
Guan, D.H., Zhang, Y.S., Al-Kaisi, M.M., Wang, Q.Y., Zhang, M.C., Li, Z.H., 2015. Tillage practices effect on root distribution and water use efficiency of winter wheat under rain-fed condition in the North China Plain. Soil Tillage Res. 146, 286–295.
Li, H.M., Inanaga, S., Li, Z.H., Eneji, A.E., 2005. Optimizing irrigation scheduling for winter wheat in the North China Plain. Agric. Water Manag. 76, 8–23.
Li, L., Sun, J.H., Zhang, F.S., Guo, T.W., Bao, X.G., Smith, F.A., et al., 2006. Root distribution and interactions between intercropped species. Oecologia 147, 280–290.
Li, F.D., Song, X.F., Tang, C.Y., Liu, C.M., Yu, J.J., Zhang, W.J., 2007. Tracing infiltration and recharge using stable isotope in Taihang Mt., North China. Environ. Geol. 53, 687–696.
Li, Q.Q., Dong, B.D., Qiao, Y.Z., Liu, M.Y., Zhang, J.W., 2010. Root growth, available soil water, and water-use efficiency of winter wheat under different irrigation regimes applied at different growth stages in North China. Agric. Water Manag. 97, 1676–1682.
Liu, C.M., Yu, J.J., Kendy, E., 2001. Groundwater exploitation and its impact on the environment in the North China Plain. Water Int. 26, 265–272.
Ma, Y., Song, X.F., 2016. Using stable isotopes to determine seasonal variations in water uptake of summer maize under different fertilization treatments. Sci. Total Environ. 550, 471–483.
Meissner, M., Kohler, M., Schwendenmann, L., Holscher, D., Dyckmans, J., 2014. Soil water uptake by trees using water stable isotopes (δ^{2}H and δ^{18}O)-a method test regarding soil moisture, texture and carbonate. Plant Soil 376, 327–335.
Mo, X.G., Xia, J., Hu, S., Lin, Z.H., 2016. Influences of climate changes on agricultural water resources in North China Plain. Chin. J. Nat. Med. 38, 189–192.
Moore, J.W., Semmens, B.X., 2008. Incorporating uncertainty and prior information into stable isotope mixing models. Ecol. Lett. 11, 470–480.
Moreno-Gutierrez, C., Dawson, T.E., Nicolas, E., Querejeta, J.I., 2012. Isotopes reveal contrasting water use strategies among coexisting plant species in a Mediterranean ecosystem. New Phytol. 196, 489–496.
Paces, J.B., Wurster, F.C., 2014. Natural uranium and strontium isotope tracers of water sources and surface water-groundwater interactions in arid wetlands - Pahranagat Valley, Nevada, USA. J. Hydrol. 517, 213–225.
Qiu, G.Y., Wang, L.M., He, X.H., Zhang, X.Y., Chen, S.Y., Chen, J., et al., 2008. Water use efficiency and evapotranspiration of winter wheat and its response to irrigation regime in the North China Plain. Agric. For. Meteorol. 148, 1848–1859.
Richards, J.H., Caldwell, M.M., 1987. A method to extract soil water for stable isotope analysis. New Phytol. 115, 379–406.
Rijsberman, F.R., 2006. Water scarcity: fact or fiction? Agric. Water Manag. 80, 5–22.
Schultz, N.M., Griffis, T.J., Lee, X.H., Baker, J.M., 2011. Identification and correction of spectral contamination in H^2/H^1 and O^{18}/O^{16} measured in leaf, stem, and soil water. Rapid Commun. Mass Spectrom. 25, 3360–3368.
Song, L.N., Zhu, J.J., Li, M.C., Zhang, J.X., Lv, L.Y., 2016. Sources of water used by *Pinus sylvestris* var. mongolica trees based on stable isotope measurements in a semiarid sandy region of Northeast China. Agric. Water Manag. 164, 281–290.
Sprenger, M., Leistert, H., Gimbel, K., Weiler, M., 2016. Illuminating hydrological processes at the soil-vegetation-atmosphere interface with water stable isotopes. Rev. Geophys. 54, 674–704.
Staff, S.S., 1999. Soil taxonomy: a basic system of soil classification for making and interpreting soil surveys. Agriculture Handbook 436. Natural Resources Conservation Service, United States Department of Agriculture (USDA), Washington, USA.
Tang, Y.K., Wen, X.F., Sun, X.M., Zhang, X.Y., Wang, H.M., 2014. The limiting effect of deep soil water on evapotranspiration of a subtropical coniferous plantation subjected to seasonal drought. Adv. Atmos. Sci. 31, 385–395.
Walter, K., 2010. Einfluss der Pflanzen auf die Isotopenzusammensetzung des Abflusses in Einzugsgebieten, Diplomarbeit, Institut für Hydrologie, Albert-Ludwigs-Universität Freiburg i. Br., Freiburg i. Br..
Wang, P., Song, X.F., Han, D.M., Zhang, Y.H., Liu, X., 2010. A study of root water uptake of crops indicated by hydrogen and oxygen stable isotopes: a case in Shanxi Province, China. Agric. Water Manag. 97, 475–482.

Wang, S.Q., Tang, C.Y., Song, X.F., Wang, Q.X., Zhang, Y.H., Yuan, R.Q., 2014. The impacts of a linear wastewater reservoir on groundwater recharge and geochemical evolution in a semi-arid area of the Lake Baiyangdian watershed, North China Plain. Sci. Total Environ. 482, 325–335.
Wu, Y., Zhou, H., Zheng, X.J., Li, Y., Tang, L.S., 2014. Seasonal changes in the water use strategies of three co-occurring desert shrubs. Hydrol. Process. 28, 6265–6275.
Wu, Y.J., Du, T.S., Li, F.S., Li, S.E., Ding, R.S., Tong, L., 2016. Quantification of maize water uptake from different layers and root zones under alternate furrow irrigation using stable oxygen isotope. Agric. Water Manag. 168, 35–44.
Xue, Q., Zhu, Z., Musick, J.T., Stewart, B.A., Dusek, D.A., 2003. Root growth and water uptake in winter wheat under deficit irrigation. Plant Soil 257, 151–161.
Yang, B., Wen, X.F., Sun, X.M., 2015. Seasonal variations in depth of water uptake for a subtropical coniferous plantation subjected to drought in an East Asian monsoon region. Agric. For. Meteorol. 201, 218–228.
Zhang, X., Chen, S., Sun, H., Wang, Y., Shao, L., 2004. Root size: distribution and soil water deletion as affected by cultivars and environmental factors. Field Crop Res. 114, 75–83.
Zhang, Y.C., Shen, Y.J., Sun, H.Y., Gates, J.B., 2011. Evapotranspiration and its partitioning in an irrigated winter wheat field: a combined isotopic and micrometeorologic approach. J. Hydrol. 408, 203–211.
Zimmermann, U., Ehhalt, D., Munnich, K.O., 1967. Soil-water Movement and Evapotranspiration: Changes in the Isotopic Composition of the Water. International Atomic Agency (IAEA): IAEA.
Zipper, S.C., Soylu, M.E., Booth, E.G., Loheide, S.P., 2015. Untangling the effects of shallow groundwater and soil texture as drivers of subfield-scale yield variability. Water Resour. Res. 51, 6338–6358.